

Caffeinated FPGAs: FPGA Framework For Convolutional Neural Networks

Roberto DiCecco*, Griffin Lacey†, Jasmina Vasiljevic*, Paul Chow*, Graham Taylor† and Shawki Areibi†

*University of Toronto, Department of Electrical and Computer Engineering, Ontario, Canada

E-mail:{dicecco1, vasiljev, pc}@eecg.toronto.edu

†University of Guelph, Ontario, Canada

E-mail:{laceyg, gwtaylor, sareibi}@uoguelph.ca

Abstract—Convolutional Neural Networks (CNNs) have gained significant traction in the field of machine learning, particularly due to their high accuracy in visual recognition. Recent works have pushed the performance of GPU implementations of CNNs to significantly improve their classification and training times. With these improvements, many frameworks have become available for implementing CNNs on both CPUs and GPUs, with no support for FPGA implementations. In this work we present a modified version of the popular CNN framework Caffe, with FPGA support. This allows for classification using CNN models and specialized FPGA implementations with the flexibility of reprogramming the device when necessary, seamless memory transactions between host and device, simple-to-use test benches, and the ability to create pipelined layer implementations. To validate the framework, we use the Xilinx SDAccel environment to implement an FPGA-based Winograd convolution engine and show that the FPGA layer can be used alongside other layers running on a host processor to run several popular CNNs (AlexNet, GoogleNet, VGG A, Overfeat). The results show that our framework achieves 50 GFLOPS across 3×3 convolutions in the benchmarks. This is achieved within a practical framework, which will aid in future development of FPGA-based CNNs.

I. INTRODUCTION

Convolutional Neural Networks (CNNs) are highly accurate deep learning networks inspired by the mammalian visual cortex. A number of works explored the implementation of CNNs on FPGAs [1]–[3] to take advantage of their low-power, customizable and programmable fabric. While FPGA implementations show promise in efficiently computing CNNs, they lack the infrastructure available for both CPUs and GPUs. This makes FPGAs inaccessible to deep learning scientists. There are many frameworks for CNN implementations, most of which provide support for CPU, GPU or the option of both [4]. These frameworks allow the programmer to launch any CNN model, and contain comprehensive tests for both layer-based and system-based executions [4]. However, none of the prominent CNN frameworks provide support for FPGA implementations. As a result, to implement a CNN on the FPGA, the designer has to manually design the implementation for each model, as well as test for correctness and optimize for performance, essentially rebuilding from scratch, rather than taking advantage of existing work.

CNNs are very computationally intensive with most of the computation in the convolution layers. The convolution layers require a large number of multiply-accumulate operations. The large computational complexity motivates efforts to reduce the

number of required operations. One approach is to use the FFT for convolution because in the frequency domain, the convolution becomes multiplication of each transformed input with the corresponding transformed filter coefficients, resulting in a compute reduction and speedup [5]. An alternative approach uses the Winograd minimal filtering algorithm to take advantage of the overlapping computations between adjacent convolution windows [6], [7]. In this work we implement and optimize the Winograd algorithm on an FPGA within the Caffe framework [4].

This paper makes the following contributions:

- We present an adaptation of the Caffe CNN framework with support for the Xilinx FPGA SDAccel environment. This adaptation allows us to launch CNN classification on CPU-FPGA-based systems.
- We describe a modification to the Winograd convolution algorithm to further reduce DSP utilization for FPGA-based implementations.
- We implement the Winograd convolution algorithm targeting any 3×3 convolution layer with unity stride and benchmark it across several popular CNNs. Results show that the architecture achieves approximately 50 GFLOPS across the 3×3 convolution layers of the benchmark suite, while using 83.2% of the available SDAccel resources in a Xilinx Virtex 7 XC7VX690T-2.
- Finally, the software and hardware implementation details have been made open-source and can be found at the following link: https://github.com/dicecco1/fpga_caffe.

This work is organized as follows: Section II provides background information on CNNs and the Xilinx SDAccel OpenCL framework. Section III discusses the Winograd convolution algorithm and FPGA implementation. Section IV details the features included in the FPGA Caffe framework and Section V shows the area utilization and performance results of the Winograd convolution engine within the FPGA Caffe framework. Section VI reviews related work and compares this work to other recent FPGA implementations. Finally, Section VII discusses future work related to the FPGA Caffe framework, and Section VIII concludes the paper.

II. BACKGROUND

The following subsections detail the necessary background information regarding CNNs and the Xilinx SDAccel OpenCL

development environment.

A. Convolutional Neural Networks

CNNs are a popular type of supervised machine learning algorithm. Similar to other machine learning algorithms, CNNs can be trained using back propagation to learn complex representations useful for many applications. CNNs are commonly used for performing object recognition in pixel-based input. A popular CNN model such as AlexNet [8] can be used to classify up to 1000 different objects in images with high accuracy.

These networks have two different modes of operation: training and inference. In the case of object recognition, training involves feeding a large number of human-annotated images into the network. These images are used by the CNN to repeatedly update the model's weights and biases such that it can learn how to recognize the objects in the human-annotated images. Classification uses the trained CNN model and presents it images that the model has never seen to attempt to predict what the object in the image is.

B. CNN Layers

AlexNet was one of the first successful ImageNet submissions employing CNNs and it consists of several layers: Convolution, Max Pooling, Fully Connected (FC), Rectified Linear Unit (ReLU), and Local Response Normalization (LRN) [8]. In many of the top performing CNNs, Convolution, Pooling, Fully Connected, and ReLU layers are typically used, while LRN and other layers are sometimes used depending on the model [8]–[11]. The general structure of a CNN usually consists of stacks of convolution layers with ReLU activations followed by a pooling layer. In recognition applications, fully connected layers are used towards the output to reduce spatially organized information into a decision. Convolution layers represent the majority of the computation for a CNN, with extreme cases requiring upwards of 30 GFLOPs of computation [9]. The ReLU layer is an activation function used to introduce a non-linearity into the network and can be described by $y = \max(0, x)$, which is applied to every data point of the input. Pooling is a simple reduction operation, such as max or average, applied to local regions of the input using a sliding window approach. FC layers consist of dense connections between neurons and usually contain the majority of the weights in the network. The computation of FC layers corresponds to a matrix multiplication followed by the addition of an optional bias parameter to each output.

C. Parallelism Strategies

Given the large computational requirements and inherent parallelism of neural networks, these architectures are ideal for hardware accelerators. Popular parallelism strategies can be reduced to three main categories.

Data Parallelism – splitting the data across different execution threads, but using the same model. For the pixel-based input (e.g. images) natural to CNNs, data parallelism is inherent given the independence of individual and local groups of pixels. Fine-grained data parallelism can be applied using

operations applied concurrently to all pixels, while coarse-grained data parallelism can be applied by processing “mini-batches” of hundreds or thousands of input images during training.

Model parallelism – splitting the model across different execution threads, but using the same data. This strategy offers several advantages, such as being able to accommodate large neural network sizes by splitting the weights across hardware accelerators, and employing a type of efficient model averaging during training.

Pipeline Parallelism – operating different dependent steps of computation concurrently on different threads, so that output from one step is streamed as input to the next, while execution of steps is overlapping. The feed-forward computation of CNNs are well suited for pipeline parallelism, so hardware that can exploit deep pipeline parallelism (e.g. FPGAs) can offer an advantage.

D. SDAccel OpenCL FPGA Programming Model

Using the SDAccel OpenCL environment to perform computations on an FPGA involves both host and kernel code. The host code is used for programming the FPGA, passing data between the host's memory and the FPGA's global memory, and launching the kernel on the FPGA. The FPGA is segmented into two regions, the programmable region and the static region. The static region is programmed upon power-up and it contains the interfaces to global memory and PCIe. The programmable region contains the kernel, the computation to be accelerated. The kernel code is synthesized into hardware and configured into the programmable region of the FPGA. The synthesized kernel can contain one or more compute units (CUs), where a CU corresponds to the hardware unit responsible for the required computation. One approach to increasing parallelism in the host code is to instantiate multiple CUs as shown in Fig. 1, with each CU handling an equally sized portion of the problem [12]. The portion of the problem handled by a single CU is referred to as the local work group size, while the size of the overall task to be completed is referred to as the global work group size. Each CU has its own local memory that is only accessible to the CU while all CUs share the global off-chip memory of the platform.

We have integrated SDAccel into the Caffe framework and used it to develop a convolution kernel using the Winograd transform.

III. WINOGRAD CONVOLUTION

Winograd convolution exploits the Winograd minimal filtering algorithm [6]. This approach has been shown to reduce the amount of required floating point operations [7]. The sections below provide an overview for the Winograd convolution algorithm and discusses the implementation details of the FPGA-based Winograd convolution engine.

A. Winograd Convolution Algorithm

The Winograd convolution algorithm output is referred to as $F(m \times m, r \times r)$. In this expression $m \times m$ refers to the output tile size for a given input tile, meaning that $m \times m$ output

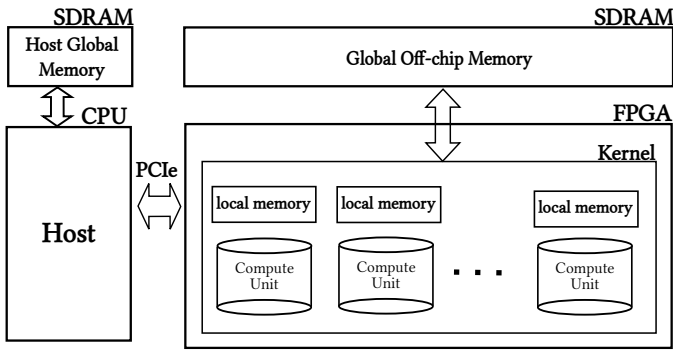


Fig. 1. SDAccel Platform

values are produced for every instance of $F(m \times m, r \times r)$. The filter size in this case is $r \times r$. For a given filter size, many different values of m can be chosen, which changes the computational complexity of $F(m \times m, r \times r)$, but does not impact the overall result. In this work, we implement a $F(2 \times 2, 3 \times 3)$ Winograd algorithm. In the case of 3×3 convolutions, $F(2 \times 2, 3 \times 3)$ has been shown to provide significant performance gains for GPU implementations in [7], though larger tile sizes may produce additional gains. This work targets $F(2 \times 2, 3 \times 3)$, mainly due to its simplicity of implementation however future work may explore other tile sizes as well. The equations for Winograd convolution are shown in Equations 1 to 3. Equation 1 shows how the filter transformation is calculated.

$$U = GgG^T \quad (1)$$

Where

- U is a $(m + r - 1) \times (m + r - 1)$ transformed filter;
- g is an $r \times r$ filter;
- G is an $(m + r - 1) \times r$ transform matrix, defined by the Winograd algorithm.

The filter values (g) are known at compile time and remain constant during run-time. Therefore, to save resources during run-time, the Winograd transformation for the filter values, shown in Equation 1, can be executed at compile time, on the CPU. This approach saves FPGA resources. However, pre-computing filter values increases the memory storage requirement. For direct convolution, the 3×3 filters require $C \times 3 \times 3$ storage, where C is the number of input channels. For Winograd-based convolution, after the transformation, the 3×3 filter is transformed into a 4×4 matrix, requiring $C \times 4 \times 4$. Therefore the storage requirement is increased by 33%.

Equation 2 shows how the input transformation is calculated.

$$V = B^T dB \quad (2)$$

Where

- V is an $(m + r - 1) \times (m + r - 1)$ transformed data tile;
- d is an $(m + r - 1) \times (m + r - 1)$ input tile;
- B is an $(m + r - 1) \times (m + r - 1)$ transform matrix, defined by the Winograd algorithm.

For $F(2 \times 2, 3 \times 3)$ input tile (d) is 4×4 and is generated by a sliding window across the 2-D input feature data. Shown in Fig. 2, the d window slides horizontally across the input data, with a stride of two. After the Winograd transformation, the 4×4 V tiles are stored back into memory. Because the input tiles contain overlaps of the input data, four times more memory storage is required.

Equation 3 shows how the pre-computed transformed filter U and the run-time transformed input data V are used to calculate the final output, a 2×2 tile Y . Each Y tile corresponds to a 2×2 non-overlapping subsection of the overall convolution output.

$$Y = F(m \times m, r \times r) = A^T[U \odot V]A \quad (3)$$

Where

- Y is an $m \times m$ output tile;
- \odot is an element wise multiplication;
- A is an $(m + r - 1) \times m$ transform matrix, defined by the Winograd algorithm.

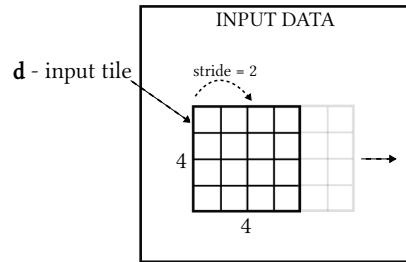


Fig. 2. Winograd Input Tile Stencil

B. FPGA Winograd Convolution

To validate the FPGA Caffe framework, efforts were primarily focused on implementing the Winograd algorithm for convolution ($F(2 \times 2, 3 \times 3)$) discussed in Section III-A, though other less optimized implementations of the layers discussed in Section II-B have been created as well. The architecture created for the Winograd algorithm on the FPGA can be separated into three stages of operation: input, compute, and output.

Input Stage – used to move the input frames from off-chip SDRAM memory to the on-chip BRAMs. A portion of the input frame is burst read into a temporary buffer through an AXI request and moved into tiles of four rows by two columns stored in BRAM. The tiles in this case deviate from the algorithm discussed in Section III-A as data is only replicated in overlapping rows of tiles rather than both overlapping rows and columns to reduce the memory overhead of storing input tiles. This tiling method is similar to the method in Fig. 2,

however while the stride stays the same, the tile width is two resulting in no overlaps. To facilitate the compute stage and output stages, the number of tiles per row is set to be a multiple of eight, with padding added as required. After tiling is completed, a portion of the Winograd input transformation shown in Equation 4 is applied to every column of the 4×2 tiles.

$$\begin{aligned}
 O[0, j] &= I[0, j] - I[2, j] \\
 O[1, j] &= I[1, j] + I[2, j] \\
 O[2, j] &= I[2, j] - I[1, j] \\
 O[3, j] &= I[1, j] - I[3, j]
 \end{aligned} \tag{4}$$

Where

$I[n, m]$ is the input of the partial transform at (n, m) ;
 $O[n, m]$ is the output of the partial transform at (n, m) .

This partial transformation is replicated eight times in the input stage such that eight columns of the input tiles can be processed per cycle to reduce the overhead that this preprocessing causes.

The full input transformation in Equation 2 requires a total of eight instances of Equation 4 per 4×4 tile, with four instances being applied to the columns, and four instances being applied to the rows of the tile (indices of Equation 4 are swapped for row calculations) as shown in Fig. 3. This results in 32 floating point additions and 64 DSPs per input tile transformation instantiation. Exploiting the fact that each input tile overlaps every two rows and every two columns with its neighbor, savings can be achieved by first precomputing either all of the column wise instances of Equation 4 or all of the row wise instances rather than computing the full transform for each tile. This reduces the number of partial transforms required for either the column wise or row wise instances from four to two per tile, which reduces the number of floating point additions to 24 from 32 per input tile transformation (with potentially one additional set of column transformations for the edge of each row).

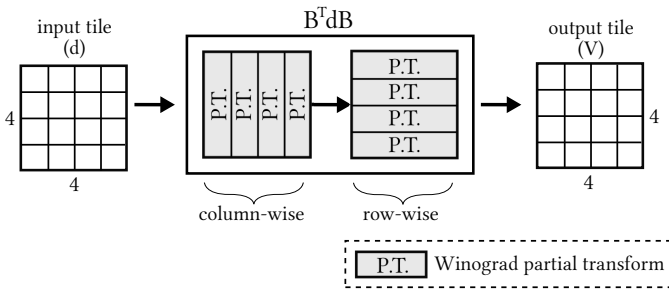


Fig. 3. Winograd Forward Transform

Compute Stage – where the bulk of the processing time is spent in the architecture. Following the input stage, each 4×2 tile and its neighbor are fed into a pipelined processing element that handles all subsequent computations required by the algorithm. The processing element completes the remaining set of partial transforms required after the input stage, performs

the element wise multiplication between the input and the weights, computes the output transform, and accumulates the result within an output buffer. This process is repeated with different weights per output feature map until all of the output feature maps have been computed. Per output feature map this requires $C \times P \times Q + D$ clock cycles, where C is the number of input channels, P is the number of output tiles per column, Q is the number of output tiles per row, and D is the number of cycles required to fill the pipeline. To reduce the cycles required per output feature map, the processing element is replicated four times, allowing this stage to effectively be completed four times faster (assuming that D is small).

Output Stage – handles transferring the output frame back into the off-chip DRR memory. First the results are gathered from the partial result buffers of the compute stage to an output buffer. Then the output is burst written to the DDR through AXI.

To further improve the performance of the engine, it has been replicated such that there are two CUs rather than one. Each CU handles a separate input image to exploit coarse-grained data parallelism. The performance of the engine is directly proportional to how many CUs can be replicated, with the execution time being dictated by the equation $T = (C \times N) / (F \times \#CUs)$, where F is the operating frequency, C is the number of clock cycles, N is the number of images, and T is the total latency.

IV. FPGA CAFFE FRAMEWORK

The Caffe framework [4] is used to describe CNNs based on predefined layer implementations with CPU and GPU backends. In this section we describe our approach to augmenting the Caffe framework to enable CNN classification using FPGAs. The discussion below will detail how memory transfers between the device and host are handled, how FPGA test benches may be used within the framework, and several FPGA specific layer implementations. The layers include a custom layer for reprogramming the FPGA and pipeline layers for fused layer implementations.

A. Caffe Model Description

The infrastructure in Caffe allows for simple description of common layers used in CNNs and provides several implementations of existing high performance CNNs as well. Each layer in Caffe corresponds to a set of computations required by a given CNN model, allowing for modular CNN implementations. Caffe also allows for networks to be defined without modification of source code by providing model definitions through the Protocol Buffer Language [4]. This allows for networks to be constructed through a file describing which layers are required and their respective ordering.

The model description format in Caffe has been augmented in this work to support additional features described in the sections below. Namely, in the FPGA Caffe framework a program layer can be specified in any position of the network to force the FPGA to be reprogrammed, pipelined layers can be specified if a fused layer is required, and the Winograd

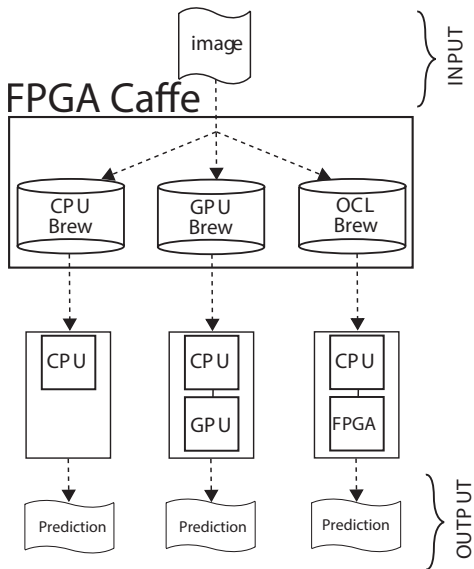


Fig. 4. High-Level View of the Brew Options in Caffe

convolution engine discussed in Section III-B can be specified when needed.

B. OpenCL Brew

In Caffe a Brew is referred to as a mode of operation that determines the target architecture on which CNN classification or training is executed. The original Brews are CPU or GPU, with the CPU Brew containing the C++ infrastructure required to define layers using a CPU, and the GPU Brew providing similar features but for NVIDIA GPUs using CUDA and cuDNN [4], [13]. For each Brew, Caffe contains test cases available for every layer, allowing for fast determination of functional correctness and benchmarking.

This work extends the baseline Caffe framework to include the OCL (OpenCL) Brew, which provides support for Xilinx FPGA-based CNNs and could easily be adapted to target Altera’s OpenCL programming environment as well. The user can choose between the different Brews by building the framework using the corresponding Makefile flags and changing the Brew to OCL. Fig. 4 shows an overview of the augmented system with the OCL Brew, where inputs and outputs are the same as in the CPU and GPU Brews, but the underlying hardware of the system is comprised of the CPU for host code and the FPGA for layer computations.

To perform a forward pass (inference) using the OCL Brew, we added an API call: `forward_ocl()`. The `forward_ocl()` API call is used as the forward operator on the condition that the Brew is OCL and the function is defined, otherwise it defaults to the `forward_cpu()` call as in the baseline Caffe implementation.

C. OpenCL Memory Management and Synchronization

Data in Caffe is represented as a four-dimensional flattened array, with allocation, resizing, and synchronization between

CPU and GPU resources abstracted from its usage [4]. The memory management API in Caffe handles synchronization between the host and GPU devices such that memory is only transferred back to the host when necessary. To accomplish this, the state of the memory is stored as either `HEAD_AT_GPU`, `HEAD_AT_CPU`, or `SYNCED` which is verified upon accessing the data. If the state of the data is `HEAD_AT_GPU` and the host requests the data, a data transfer from the device to the host will be issued and the state will change to `SYNCED`.

Support for memory synchronization between the host and the FPGA in the FPGA Caffe framework builds on the memory synchronization features described above. To accomplish similar functionality, OpenCL APIs are used with an additional object corresponding to the FPGA device memory object for each data structure. When data is passed from the host to the FPGA, the state of the memory changes to `HEAD_AT_OCL` such that on subsequent accesses it will either stay in the device memory or be transferred back to host memory. If the data is required by the host, a memory transfer will be issued from the device to the host and the state of the memory will change to `SYNCED`. To access the FPGA memory object, calls to either `mutable_ocl_data()` for modifying data (layer output data) or `ocldata()` for static data (layer input data, such as weights), are required. These two functions were added to Caffe to handle both the creation and synchronization of the device and host memory while maintaining transparency of memory manipulation as in the baseline Caffe implementation.

D. FPGA Testbenches

Testing a given layer in the FPGA framework can be accomplished in two different ways depending on the stage of development. Layers can be tested using individual test cases through the test framework provided in Caffe. Alternatively they can also be tested through the use of standalone host code by invoking only the host code required to launch the kernel. In either case, the layer can be tested using a hardware implementation or using software emulation based implementations created in the Xilinx SDAccel environment.

The baseline Caffe framework has a number of tests that are available for each layer of the system [4]. Each test can be made into a test for the FPGA implementations by changing the Brew to OCL and modifying parameters to suit a given layer. These tests allow for larger scale testing to verify that the layer has been integrated properly within the Caffe framework. Aside from providing breadth to the test suite, this also allows for fast prototyping of layers through the use of software emulated layers provided by the capabilities of SDAccel [12].

E. Kernel Compilation

Compiling kernels for CPUs and GPUs amounts to compiling programs into instructions that program the hardware, whereas compiling for FPGAs involves synthesizing full circuits. As a result, the overhead of compilation for FPGAs (hours) is much greater than that of CPUs and GPUs (milliseconds), and so runtime compilation of FPGA kernels is not possible. We deal with this problem by employing an

offline compilation strategy, where deep learning practitioners can make use of precompiled binaries at run-time.

F. XCLProgram Layer

Though FPGA Caffe makes use of offline binary compilation, there is still significant overhead from programming the FPGA (100-300 ms) compared to the CPU and GPU (0.001-0.005 ms). This programming overhead conflates the measured execution time for a layer in the Caffe benchmarking functionality. We introduce a new layer, the XCLProgram layer, as a method for giving the user greater control over how the FPGA is programmed, as well as the ability to separately benchmark the execution time of each layer and programming overhead. The XCLProgram layer as input receives a pointer to the FPGA binary file, as well as the kernel name.

G. Pipelined Layers

In the GPU-based approach native to Caffe, modularity is enforced layer-wise, meaning before each layer is executed the GPU is programmed with the appropriate kernel and memory is synchronized with the host. In FPGA Caffe this becomes a bottleneck given the large overhead of programming the FPGA, and requiring such frequent memory synchronization with the host is much more expensive on FPGAs compared to high memory bandwidth GPUs. Additionally, this modularity used in Caffe limits parallelism strategies to within each kernel. To address these issues, we introduce a new layer type in FPGA Caffe called pipeline layers. Facilitated by XCLProgram layers, pipeline layers package multiple kernels into a single binary, with kernel-kernel communication occurring through local memory structures on the FPGA (i.e. FIFO). Pipeline layers reduce the number of times the FPGA is programmed, and eliminate the need to synchronize memory with the host between every layer. Most importantly, pipeline layers allow pipeline parallelism strategies across layers, increasing throughput by allowing multiple layers to execute concurrently. While the use of pipeline layers violates some modularity assumptions of Caffe, we argue that this is practical given that combinations of layer groups are very predictable in practice (e.g. convolution, ReLU, pooling).

V. RESULTS

This section describes our study of the Winograd Convolution Algorithm and the results gathered from using FPGA Caffe to implement the 3×3 convolution layer using the Winograd Convolution Algorithm. The platform we use includes an Alpha-Data ADM-PCIE-7V3 card with a Xilinx Virtex 7 XC7VX690T-2 running at 200 MHz and an Intel Xeon CPU E5-2620 running at 2.0 GHz for the host application code. The Xilinx Virtex 7 is contained within a server that has been virtualized to support virtual machines (VM) and is connected through PCIe. The VM in use has 8GB RAM and four cores. An Intel i7-4770k running at 3.5 GHz was used for CPU comparison and an nVidia Quadro K620 for GPU comparisons. The Xilinx SDAccel version number is 2015.1.3, CUDA version number is 7.5, cuDNN version number is 4.0 [13] and the CPU host code uses OpenBLAS [14] with eight threads

enabled. The CPU, GPU, and FPGA implementations all use single precision floating point as their data representation.

A. Winograd Resource Utilization

The resource utilization post place and route is shown in Table I. The highest utilization post place and route for both CUs is the LUT utilization at 83.2% of the SDAccel region's available LUTs. The utilization post place and route accounts for additional resources required to integrate into the SDAccel framework, which drives the significant LUT utilization in comparison to other resources on the device.

TABLE I
SINGLE PRECISION WINOGRAD CONVOLUTION ENGINE RESOURCE UTILIZATION POST PLACE AND ROUTE

	FF	LUT	DSP	BRAM (18Kb)
-				
XC7VX690T				
Total Resources (A)	866,400	433,200	3,600	2,940
SDAccel Region (B)	551,040	275,520	2,376	1,940
Winograd				
Conv. Engine (C)	253,873	229,226	1,307	1,188
SDAccel				
Utilization (C/B)	46.7%	83.2%	55%	61.2%
Total				
Device Utilization (C/A)	29.3%	52.9%	36.3%	40.4%

Given the utilization of the device resources, further instances of the CU could theoretically be added, though the limits on the available resources in the SDAccel region of the FPGA shown in Table I makes it impossible to place more than two CUs. This in turn limits the potential performance of the architecture within the SDAccel environment because of the overhead of the static region and the lack of resources available in the reconfigurable region.

To quantify the DSP savings from using the input stage column transformation discussed in Section III-B we consider three separate cases. The first case is that the full input transform is pre-computed for each four by four tile before sending the data to the processing elements of the compute stage, with only one instance of the full input transformation in Equation 2. The second case is that the full input transformation in Equation 2 is computed within each processing element of the compute stage using one full input transformation per processing element. Finally, the last case is the one discussed in Section III-B, in which a column-wise partial transformation is computed for all input tile columns, using eight partial transformations to reduce computation overhead, with the remaining partial transformations computed within the processing elements using four partial transformations per processing element. Table II shows the resource utilization of the three cases post place and route. Between cases 2 and 3 there is a DSP savings of 61 units and a decrease in LUT usage. This is slightly less than what is anticipated in Section III-B, though the difference can be attributed to fewer addressing calculations being required in case 2 due to the elimination of the partial transformations in the input stage. When comparing with case 1, the DSP utilization is approximately 20% less than case 3, however the BRAM utilization

has increased by 33% due to the storing of replicated data in overlapping tiles. While the LUT usage and DSP utilization is better in case 1, the BRAM utilization makes it difficult to place and route more than 1 CU, as the BRAM utilization for two would require most of the available BRAM.

TABLE II
RESOURCE UTILIZATION FOR DIFFERENT WINOGRAD STRATEGIES WITH ONE CU

Layer	FF	LUT	DSP	BRAM (18Kb)
Case 1: Full Pre-Transform	143,965	127,989	523	914
Case 2: Full Transform in PE	166,905	153,887	715	688
Case 3: Partial Transform in PE	158,266	145,892	654	688

B. FPGA Caffe Benchmark Results

To evaluate the Winograd convolution engine within the FPGA Caffe framework, a set of benchmark CNNs is required to view its performance across varying workloads (number of output feature maps and output sizes). The benchmark suite that we use is adopted from the Soumith Chintala convnet-benchmarks [15], which is composed of previous ImageNet winners including: AlexNet [8], VGG A [9], Overfeat [10], and GoogleNet [11]. Due to the RAM size of the virtual machine used for the host code, the batch size for each benchmark is reduced by half to fit within the host VM.

Table III shows the performance of the system in comparison to both CPU and GPU implementations of the 3×3 convolution layers of each CNN. To calculate the GFLOPS of the Winograd convolution engine, the number of floating-point operations is taken to be the same as direct convolution, as is the case in [7], which is considered to be the effective GFLOPS. Comparing the geometric averages in Table III, the Winograd convolution engine performs approximately 2.1 times slower than the CPU implementation and 9.4 times slower than the GPU implementation.

VI. RELATED WORK

There exist several frameworks for implementing CNNs depending on the targeted platform and programming language, with many of the popular frameworks discussed in [4]. These frameworks typically support a number of programming languages including: C/C++, Matlab, Python, etc. With respect to Caffe, there is an independent effort underway to add OpenCL support [16], though this support is meant primarily for exposing more GPUs to Caffe rather than FPGAs. The work in [16] provides additional functionality to support AMD devices through OpenCL and provides some similar features to those explored in this work. However, these works are differentiated in that the OpenCL implementations are abstracted away from being GPUs in this work through a separate Brew for OpenCL to allow for implementations across many different compute engines. Additionally, given the non-standard development model currently supported in FPGA OpenCL tools, frameworks that support standard OpenCL will not work with

FPGAs without significant framework modification. This is the case primarily because the FPGA OpenCL tools require offline compilation of kernels and vendor-specific attributes to achieve suitable performance. The framework introduced in this paper allows for the support of FPGAs through layer-specific implementations. These include the ability to specify when to program the FPGA, the addition of pipelined layers, and precompiled FPGA-specific layer implementations.

Table IV shows the performance of this work compared to several recent FPGA works. The highest performing implementations are Qiu [3] and Suda [2], which is enabled by their use of fixed point representations. The work of Zhang [1] is approximately 1.2-fold higher performance than this work while using the same data representation, though as expected our DSP utilization is significantly lower while achieving comparable throughput. While the performance of this implementation is lower, it does not require precision analysis prior to usage and it does not need to be resynthesized for new work loads as is the case in all of the prior works.

VII. FUTURE WORK

Future work related to this framework will contribute to both performance and usability. First, completing the implementation of back propagation will ensure FPGAs can be used for both classification and training, where hardware acceleration is especially important. Given the modularity between the solver, network, and layer in Caffe, only the layers need to be modified to accommodate backward propagation. The structure of the network that defines the collection of layers, as well as the operation of the solver that calls the backward methods to generate gradients and perform a weight update, is already in place.

As well, experimenting with reduced-precision implementations of common layers is an important next step. Recently, GPUs have started to support half precision based implementations of CNNs [7], [13] and many of the FPGA works have been focused on reduced precision implementations [2], [3]. Half precision or fixed-point implementations both would offer significant area gains for FPGA implementations as shown in [2], [3], as a floating-point multiplication requires three DSP units and additional LUTs and flip-flops for current Xilinx FPGAs, while half precision or fixed-point multiplications require only one DSP unit and significantly fewer LUTs and flip-flops. This would allow for the replication of both processing elements and CUs to improve performance.

Finally, multi-FPGA-based parallelism strategies are crucially important in scaling up to accommodate larger data and model sizes. Current solutions involve using GPU clusters with Infiniband interconnects and MPI, which allow fast node to node data transfer and increase parallelism capabilities [17]. The use of FPGAs are attractive in this domain given the flexibility and high performance/watt, and FPGAs can benefit from much of the work being done investigating multi-GPU parallelism strategies.

TABLE III
CPU, GPU, AND FPGA 3×3 CONVOLUTION BENCHMARK RESULTS

Network	CPU Run Time (ms)	GPU Run Time (ms)	FPGA Run Time (ms)	CPU GFLOPS	GPU GFLOPS	FPGA GFLOPS
AlexNet (64 Images)	492	261.2	1,010	94	177.1	45.8
VGG A (32 Images)	4,310	745.14 ^a	8,713	111.2	642.9	55
Overfeat (64 Images)	2,030	387.1	4,781	139.2	730.2	59.1
GoogleNet (64 Images)	1,506	209.66 ^b	2,937	81.8	587.8	42
Geometric Average	1,595.6	354.51	3,333.9	104.46	470.17	50

^a GPU memory could only fit 8 images, so the model was run with 8 images and execution time was multiplied by 4 to get a performance estimate.

^b GPU memory could only fit 32 images, so the model was run with 32 images and execution time was multiplied by 2 to get a performance estimate.

TABLE IV
COMPARISON BETWEEN EXISTING FPGA WORKS

Metric	Zhang [1]	Suda [2]	Qiu [3]	This Work
Clock Frequency (MHz)	100	120	150	200
Precision	32 bit float	8-16-bit fixed	16-bit fixed	32 bit float
FPGA Version	Virtex 7 VX485T	Stratix-V GSD8	Zynq XC7Z045	Virtex 7 XC7VX690T-2
DSP Utilization	2,240	(Not specified)	780	1,307
Host Connection	Microblaze, on chip host	PCIe	ARM Cortex-A9 Processor, on chip host	PCIe
GFLOPS/GOPS	61.62	136.5	187.8	50

VIII. CONCLUSION

In this work we presented a framework for implementing CNNs using FPGAs based on the Caffe CNN framework. The framework allows for transparent support for individual FPGA implementations of layers for testing and verification. This framework was validated by implementing the Winograd convolution layer and testing it across several CNNs. The results show that with 83.2% of the available SDAccel resources we are able to achieve 50 GFLOPs across the 3 × 3 convolution layers of four different CNNs. While this does not improve upon current implementations in terms of performance, it demonstrates the capabilities of the framework, which allows for further work that could lead to higher performance.

ACKNOWLEDGMENT

The authors would like to thank Xilinx, CMC and em-SYSCAN, NSERC, and CFI for the funding and resources provided for this work.

REFERENCES

- [1] Chen Zhang, Peng Li, Guangyu Sun, Yijin Guan, Bingjun Xiao, and Jason Cong. Optimizing FPGA-based Accelerator Design for Deep Convolutional Neural Networks. In *Proceedings of the 2015 ACM/SIGDA International Symposium on Field-Programmable Gate Arrays*, FPGA '15, pages 161–170, New York, NY, USA, 2015. ACM.
- [2] Naveen Suda, Vikas Chandra, Ganesh Dasika, Abinash Mohanty, Yufei Ma, Sarma Vrudhula, Jae-sun Seo, and Yu Cao. Throughput-Optimized OpenCL-based FPGA Accelerator for Large-Scale Convolutional Neural Networks. In *Proceedings of the 2016 ACM/SIGDA International Symposium on Field-Programmable Gate Arrays*, FPGA '16, pages 16–25, New York, NY, USA, 2016. ACM.
- [3] Jiantao Qiu, Jie Wang, Song Yao, Kaiyuan Guo, Boxun Li, Erjin Zhou, Jincheng Yu, Tianqi Tang, Ningyi Xu, Sen Song, Yu Wang, and Huazhong Yang. Going Deeper with Embedded FPGA Platform for Convolutional Neural Network. In *Proceedings of the 2016 ACM/SIGDA International Symposium on Field-Programmable Gate Arrays*, FPGA '16, pages 26–35, New York, NY, USA, 2016. ACM.
- [4] Yangqing Jia, Evan Shelhamer, Jeff Donahue, Sergey Karayev, Jonathan Long, Ross Girshick, Sergio Guadarrama, and Trevor Darrell. Caffe: Convolutional Architecture for Fast Feature Embedding. *arXiv preprint arXiv:1408.5093*, 2014.
- [5] Michaël Mathieu, Mikael Henaff, and Yann LeCun. Fast Training of Convolutional Networks through FFTs. *CoRR*, abs/1312.5851, 2013.
- [6] S. Winograd. *Arithmetic Complexity of Computations*. CBMS-NSF Regional Conference Series in Applied Mathematics. Society for Industrial and Applied Mathematics, 1980.
- [7] Andrew Lavin. Fast Algorithms for Convolutional Neural Networks. *CoRR*, abs/1509.09308, 2015.
- [8] Alex Krizhevsky, Ilya Sutskever, and Geoffrey E. Hinton. ImageNet Classification with Deep Convolutional Neural Networks. In F. Pereira, C.J.C. Burges, L. Bottou, and K.Q. Weinberger, editors, *Advances in Neural Information Processing Systems 25*, pages 1097–1105. Curran Associates, Inc., 2012.
- [9] K. Simonyan and A. Zisserman. Very Deep Convolutional Networks for Large-Scale Image Recognition. *CoRR*, abs/1409.1556, 2014.
- [10] Pierre Sermanet, David Eigen, Xiang Zhang, Michaël Mathieu, Rob Fergus, and Yann LeCun. OverFeat: Integrated Recognition, Localization and Detection using Convolutional Networks. *CoRR*, abs/1312.6229, 2013.
- [11] Christian Szegedy, Wei Liu, Yangqing Jia, Pierre Sermanet, Scott E. Reed, Dragomir Anguelov, Dumitru Erhan, Vincent Vanhoucke, and Andrew Rabinovich. Going Deeper with Convolutions. *CoRR*, abs/1409.4842, 2014.
- [12] Xilinx Inc. SDAccel Development Environment User Guide, September 2015.
- [13] Sharan Chetlur, Cliff Woolley, Philippe Vandermersch, Jonathan Cohen, John Tran, Bryan Catanzaro, and Evan Shelhamer. cuDNN: Efficient Primitives for Deep Learning. *CoRR*, abs/1410.0759, 2014.
- [14] Z. Xianyi, W. Qian, and Z. Yunquan. Model-driven Level 3 BLAS Performance Optimization on Loongson 3A Processor. In *Parallel and Distributed Systems (ICPADS)*, 2012 *IEEE 18th International Conference on*, pages 684–691, Dec 2012.
- [15] Soumith Chintala. Convnet-benchmarks. [Online]. Available: <https://github.com/soumith/convnet-benchmarks>.
- [16] Fabian Tschopp. Efficient Convolutional Neural Networks for Pixelwise Classification on Heterogeneous Hardware Systems. *CoRR*, abs/1509.03371, 2015.
- [17] Adam Coates, Brody Huval, Tao Wang, David Wu, Bryan Catanzaro, and Ng Andrew. Deep learning with COTS HPC systems. In *Proceedings of the 30th International Conference on Machine Learning (ICML-13)*, pages 1337–1345, 2013.